

Structure characteristics and lithium ionic conductivity of $\text{La}_{(0.57-2x/3)}\text{Sr}_x\text{Li}_{0.3}\text{TiO}_3$ perovskites

G. X. WANG*, P. YAO, D. H. BRADHURST, S. X. DOU, H. K. LIU

Energy Storage Materials Program, Institute for Superconducting and Electronic Materials, University of Wollongong, NSW 2522, Australia

E-mail: gw14@uow.edu.au

$\text{La}_{(0.57-2x/3)}\text{Sr}_x\text{Li}_{0.3}\text{TiO}_3$ perovskites were synthesised using a conventional solid-state reaction. Large Sr^{2+} ions partially substituting for La^{3+} ions were found to disturb the cubic perovskite structure and cause the superstructure lines to gradually decrease in the x-ray diffraction patterns and almost disappear when $x = 0.12$. On the contrast, there still exist superstructure diffraction spots in the electron diffraction pattern on microdomain when $x = 0.12$. The lithium ion conductivities of the compounds were improved in the range of $0 \leq x \leq 0.08$, which does not obey the principle of the carrier concentration. An expansion of the unit cell and the disordering of La^{3+} (Sr^{2+}), Li^+ ions and vacancies in A sites could be a mechanism for the enhancement of the conductivity with Sr^{2+} doping. © 2000 Kluwer Academic Publishers

1. Introduction

Lithium ion conductors have recently captured a worldwide attention because of their potential application as solid electrolytes for the solid state rechargeable lithium battery. ABO_3 perovskites and NASICONs have been investigated and demonstrated an ionic conductivity from $10^{-3} \text{ S cm}^{-1}$ to $10^{-6} \text{ S cm}^{-1}$ [1–5]. The best lithium ion conductors were found to be $\text{La}_{0.67-x}\text{Li}_{3x}\text{TiO}_3$ perovskites with a cation deficiency at A-sites [6]. The mechanism for ion conduction in ABO_3 perovskites is considered to originate from lithium ions hopping through the wide square planar bottlenecks between A-sites [7–10]. Therefore, lithium ion conductivity depends on the concentration of the free volume, lithium ion and vacancy in the A-site. It has been reported that the substitution of ions with a large ionic radius such as Sr^+ for La^{3+} ions in A-sites can increase the conductivity of ABO_3 perovskites [11, 12].

In this investigation, Sr^{2+} ion was chosen to partially substitute La^{3+} in $\text{La}_{0.57}\text{Li}_{0.3}\text{TiO}_3$ perovskite according to the principle of $\text{Sr}^{2+} = \frac{2}{3}\text{La}^{3+}$. A series of $\text{La}_{(0.57-2x/3)}\text{Sr}_x\text{Li}_{0.3}\text{TiO}_3$ perovskites were prepared and their structures and ionic conductivities were characterised.

2. Experimental

The A-site deficient $\text{La}_{(0.57-2x/3)}\text{Sr}_x\text{Li}_{0.3}\text{TiO}_3$ perovskites ($x = 0, 0.04, 0.08, 0.12$) were prepared using the solid-state reaction method. The starting materials of Li_2CO_3 (99%), La_2O_3 (99.9%), SrCO_3 (99.9%) and TiO_2 (99.7%, Anatase) from the Aldrich Chemical Co. were mixed using an agate pestle and mortar. The mix-

tures were calcined at 1100°C for 12 hours with several stages of intermediate grinding. The powders were pressed into pellets (diameter $\phi = 10 \text{ mm}$) at a pressure of 300 MPa. The pellets were sintered at 1380°C for 2 hr in air.

Powder x-ray diffraction was employed to identify phases and determine lattice parameters with a diffracted beam monochromator curved crystal (graphite 002) and Cu-K_α radiation using a MO3XHF²² diffractometer (MaCScience Co., Ltd., Japan). Silicon powder was used as an internal standard. Electron diffraction was carried out on a JEOL 2000 FX electron microscope.

The ionic conductivity of the sample was measured by an AC impedance technique using an EG&G Electrochemical Impedance Analyser (EG&G Instruments, Princeton Applied Research). The sintered samples were polished and gold was sputtered on both sides.

3. Results and discussion

The phases of the synthesised $\text{La}_{(0.57-2x/3)}\text{Sr}_x\text{Li}_{0.3}\text{TiO}_3$ were determined by powder x-ray diffraction. As shown in Fig. 1, well defined crystallinities were obtained and no impurity phases were detected by the x-ray diffraction technique, which indicates that Sr ions entered into the perovskite structure. All reflections in four samples were indexed as a cubic unit cell (space group: P4/mmm ; $c = 2a$). The superstructure lines were observed and indexed as $(hkl/2)$. These superstructure lines were generally considered to originate from the superlattice with the stacking of two perovskite sub-cells along the c axis and the ordering of La^{3+} (Sr^{2+}),

* Author to whom all correspondence should be addressed.

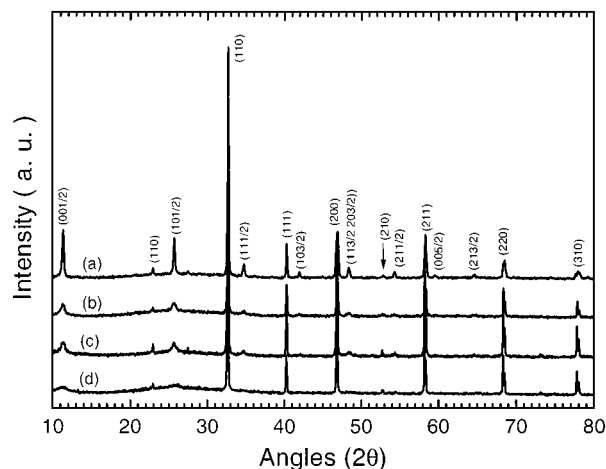


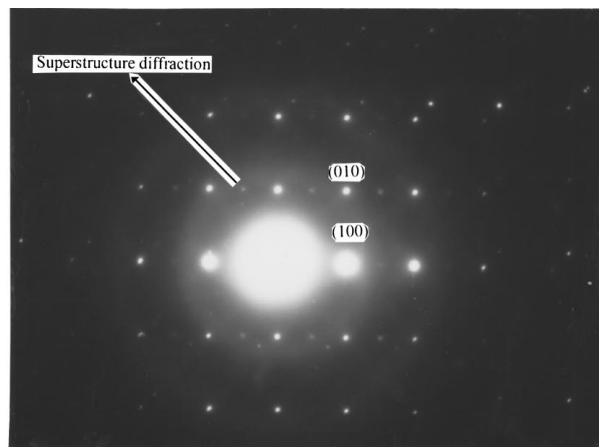
Figure 1 XRD patterns of $\text{La}_{(0.57-2x/3)}\text{Sr}_x\text{Li}_{0.3}\text{TiO}_3$ perovskites. (a) $x = 0$ (b) $x = 0.04$ (c) $x = 0.08$ (d) $x = 0.12$.

Li^+ or vacancies. With the increase of Sr content in the perovskite structure, all of the superstructure lines gradually become weak and broaden. When $x = 0.12$, all superstructure lines almost disappear. This is the first time to observe that Sr addition disturbed the superstructure of $\text{La}_x\text{Li}_y\text{TiO}_3$ perovskite. The ionic radii for Sr^{2+} and La^{3+} are 1.44 Å and 1.36 Å respectively. In the perovskite structure, A-site is tolerant to different sizes of ions. Therefore, the lattice distortion caused by the mismatch between Sr^{2+} and La^{3+} should not be the mechanism for above observation. However, the disordering of La^{3+} (Sr^{2+}), Li^+ and vacancies in the A-sites could contribute to the decreasing and broadening of the superstructure lines ($hk1/2$) in the XRD patterns.

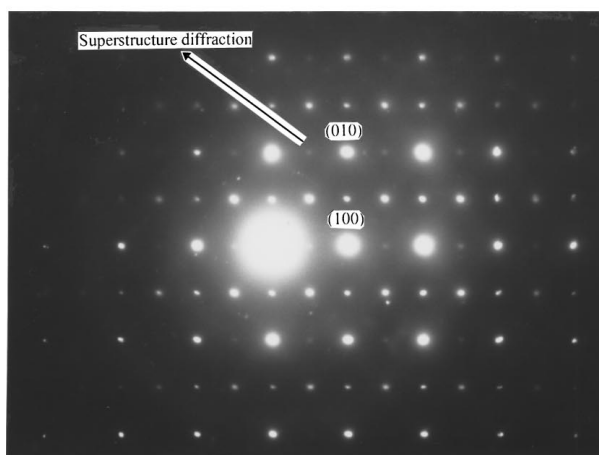
In order to observe the superlattice of $\text{La}_{(0.57-2x/3)}\text{Sr}_x\text{Li}_{0.3}\text{TiO}_3$ perovskites on microdomain, electron diffraction was performed on the powders of the perovskites. Fig. 2 shows the electron diffraction patterns of $x = 0$ and $x = 0.12$ respectively. Surprisingly, the superstructure diffraction spots were still observed when Sr addition is $x = 0.12$. This is contrast to the XRD observation, suggesting that a sub-superlattice still exists on the microdomain. In Fig. 2b, the electron diffraction pattern of superstructure is more complicated than that of $\text{La}_{0.57}\text{Li}_{0.3}\text{TiO}_3$, indicating that the addition of Sr does disturb the ordering structure of $\text{La}_{0.57}\text{Li}_{0.3}\text{TiO}_3$ perovskite.

At this stage, we can not determine the exact position of La^{3+} , Sr^{2+} , Li^+ and vacancies in the perovskite structure. Further identification needs to be done by neutron scattering. The lattice parameters of $\text{La}_{(0.57-2x/3)}\text{Sr}_x\text{Li}_{0.3}\text{TiO}_3$ perovskites were refined against an internal silicon standard using the least square method. The lattice constant a for $\text{La}_{0.57}\text{Li}_{0.3}\text{TiO}_3$ is 3.8712 Å, which is in agreement with the literature value [3]. The lattice parameters and the volume of the unit cell increase slightly with the addition of large Sr^{2+} ions (see Fig. 3). This effect would be beneficial for lithium ion diffusion.

Fig. 4 compares the lithium ionic conductivity of $\text{La}_{(0.57-2/3x)}\text{Sr}_x\text{Li}_{0.3}\text{TiO}_3$ at 25°C. The improvement of the bulk ionic conductivity was observed with the Sr^{2+}



(a)



(b)

Figure 2 Electron diffraction patterns of $\text{La}_{(0.57-2x/3)}\text{Sr}_x\text{Li}_{0.3}\text{TiO}_3$ perovskites indexed on the basis of the cubic perovskite phase. (a) $x = 0$, [001] zone axis. (b) $x = 0.12$, [001] zone axis.

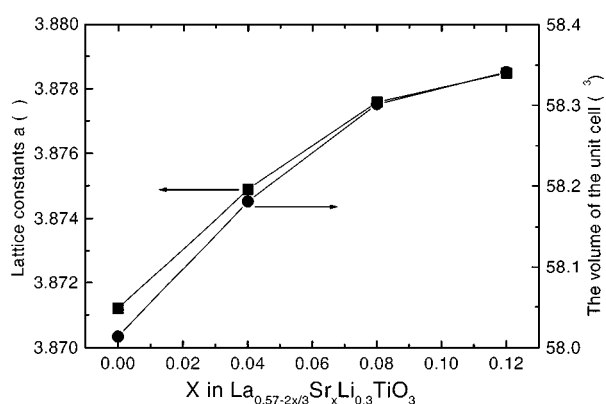


Figure 3 The lattice parameters a and the volume of the unit cell for $\text{La}_{(0.57-2x/3)}\text{Sr}_x\text{Li}_{0.3}\text{TiO}_3$.

doping effect. When $x = 0.08$, the bulk conductivity reached the maximum of $1.12 \times 10^{-3} \text{ S cm}^{-1}$.

The conductivity of the solid electrolyte is related to the carrier concentration as [6, 7]:

$$\sigma = Z_e \times C \times \mu \quad (1)$$

where Z_e is the ionic charge ($Z = 1$), C is the carrier concentration, and μ is the the mobility of lithium ions

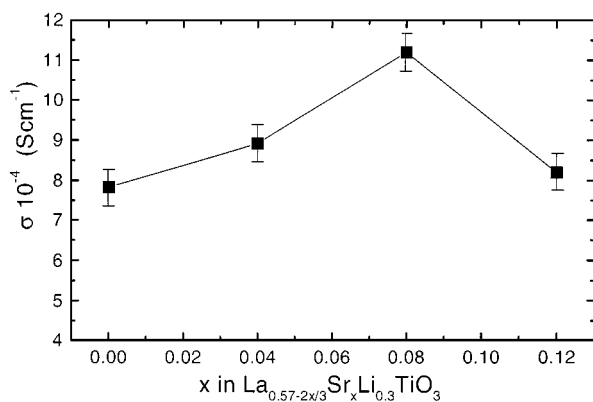


Figure 4 Lithium ion conductivity of $\text{La}_{(0.57-2x/3)}\text{Sr}_x\text{Li}_{0.3}\text{TiO}_3$ perovskites at 25 °C.

which is assumed to be constant in the certain composition range. In $\text{La}_{(0.57-2/3x)}\text{Sr}_x\text{Li}_{0.3}\text{TiO}_3$ solid solutions, the lithium ion concentration $N_{\text{Li}} = 0.3/V_s$ and vacancies $N_v = (0.13 - x/3)/V_s$ (V_s is the volume of the cubic unit cell). So, the concentration of all available A-sites for conduction is $N = N_{\text{Li}} + N_v$. Therefore, the bulk conductivity can be expressed as:

$$\begin{aligned}\sigma &= Z_e \times N_{\text{Li}}N_v/N \times \mu \\ &= Z_e \times (0.117 - 0.3x)/(1.29 - x)V_s \times \mu \quad (2)\end{aligned}$$

The vacancies decrease with the increase of x in $\text{La}_{(0.57-2/3x)}\text{Sr}_x\text{Li}_{0.3}\text{TiO}_3$ perovskite. The substitution must be limited to be $x \leq 0.39$. In this range, according to the Equation 2, the conductivity should decrease with the increase of the amount of Sr^{2+} ions. However, the experimental observation was opposite (as shown in Fig. 4). Two other factors could also contribute to the lithium ion conductivity. The increase of the unit cell volume is helpful for lithium ion diffusion. On the other hand, the disordering of La^{3+} (Sr^{2+}), Li^+ and vacancies in the A-site can also enhance lithium ion conductivity. Long-range, ionic conduction in perovskite compounds seems to involve Li ion migration through the whole bulk in three-dimensions. The ordered arrangement of La^{3+} (Sr^{2+}), Li^+ and vacancies in the A-site decreases the lithium ionic conductivity due to the block effect of large La^{3+} (Sr^{2+}) ions. In Fig. 1, the superstructure lines gradually diminish with the increase in the amount of Sr^{2+} dopant. This phenomenon suggests that the degree of the ordering of La^{3+} (Sr^{2+}), Li^+ and vacancies in A-site decreases. Consequently, the ionic conductivity could be enhanced by this effect and would therefore not obey the Equation 2.

4. Conclusions

Single phase $\text{La}_{(0.57-2x/3)}\text{Sr}_x\text{Li}_{0.3}\text{TiO}_3$ solid solutions were obtained in the range of $x \leq 0.12$. It was found that the XRD diffraction peaks of the superstructure lines ($hkl/2$) decrease gradually with the addition of large Sr^{2+} ions, which is related to the disordering of La^{3+} (Sr^{2+}), Li^+ ions and vacancies in A-sites on macroscopy. Whereas, electron diffraction observation revealed that a sub-superlattice still existed on the microdomain even when Sr addition reached $x = 0.12$. The lithium conductivity could be improved by adding Sr^{2+} ions. The maximum conductivity at room temperature is $1.12 \times 10^{-3} \text{ S cm}^{-1}$ for $x = 0.08$. This Sr^{2+} doped perovskite could be a candidate material as electrolyte for solid state lithium batteries.

Acknowledgements

G. X. Wang thanks for Dr. Ionsecu Mihail and Dr. X. L. Wang for the analysis of XRD patterns. Financial support from Department of Education, Training and Youth Affairs, Australia is gratefully acknowledged.

References

1. Y. INAGUMA, L. CHEN, M. ITOH and T. NAKAMURA, *Solid State Communications* **86** (1993) 689.
2. M. MORALES and A. R. WEST, *Solid State Ionics* **91** (1996) 33.
3. Y. HARADA, T. ISHIGAKI, H. KAWAI and J. KUWANO, *ibid.* **108** (1998) 407.
4. A. G. BELOUS, *ibid.* **90** (1996) 193.
5. B. V. R. CHOWDARI, K. RADHAKRISHNAN, K. A. THOMAS and G. V. SUBBA RAO, *Mat. Res. Bull.* **24** (1989) 221.
6. H. KAWAI and J. KUWANO, *J. Electrochem. Soc.* **141** (1994) L78.
7. Y. INAGUMA and M. ITOH, *Solid State Ionics* **86/88** (1996) 257.
8. O. BOHNKE, C. BOHNKE and J. L. FOURQUET, *ibid.* **91** (1996) 21.
9. O. BOHNKE, J. EMERY, A. VERON, J. L. FOURQUET, J. Y. BUZARE, P. FLORIAN and D. MASSIOT, *ibid.* **109** (1998) 25.
10. Y. INAGUMA, J. YU, Y. J. SHAN, M. ITOH and T. NAKAMURA, *J. Electrochem. Soc.* **L8** (1995).
11. K. NOMURA and S. TANASE, *Solid State Ionics* **98** (1997) 229.
12. Y. KAWAKAMI, M. FUKUDA, H. IKUTA and M. WAKIHARA, *ibid.* **110** (1998) 187.

Received 13 September 1999
and accepted 22 February 2000